

**СООБЩЕНИЯ  
ОБЪЕДИНЕННОГО  
ИНСТИТУТА  
ЯДЕРНЫХ  
ИССЛЕДОВАНИЙ  
ДУБНА**

**E7-84-690**

**P.Mädler**

**ON PARTICLE EMISSION  
IN TDHF APPROXIMATION**

**1984**



## 1. INTRODUCTION

Experimental data on nucleon emission from heavy ion reactions show that mechanisms other than evaporation are present in these reactions. In fact, the high-energy part of the emitted-nucleon spectra considerably exceeds the predictions of the evaporation calculations. These non-evaporation nucleons exhibit a forward-peaked angular distribution.

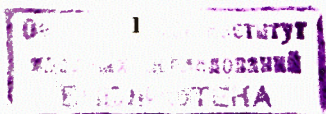
Several models have been proposed to explain these features. We mention here only:

i) The Fermi-jet model or the model of promptly emitted particles<sup>/1-3/</sup> (PEP) which describes the emission of highly energetic particles by a direct coupling between the relative velocity of the interacting heavy ions and the intrinsic Fermi motion. Owing to the long mean free path in the initially cold nuclei particles are assumed to pass freely through the recipient nucleus. On the same footing inertially emitted particles (IEP) have been investigated<sup>/4/</sup> which can be interpreted as some classical equivalent of the quantum break-up emission.

ii) Several modifications of the exciton model<sup>/5,6/</sup> and the modified Harp-Miller-Berne model<sup>/7/</sup> (which allow nucleon-nucleon rescattering via a residual interaction), i.e. do not assume quasi-freedom.

In the Fermi-jet theory PEP are too strongly focused into the forward direction and do not fit the experimental energy distributions at highest energies.

In refs.<sup>/8,9/</sup> the question was investigated if these failures are simply due to the calculation of the emission process by classical trajectories ignoring quantum diffraction. The time-dependent single-particle Schrödinger equation was solved for an initial Gaussian wave packet moving inside a Woods-Saxon potential towards the edge of the potential well. Velocity  $v_0$  and standard deviation of the initial wave packet could be chosen so that energy and angular distributions calculated from the outgoing probability flux came close to the experimental data up to an overall normalization factor.





This fit, however, led to  $v_0$  values substantially smaller than the incident projectile velocity in the considered experiment. From this it was concluded that either the ions strongly slow down prior to injection of PEP into the recipient or the assumption of quasi-freedom is wrong. There are some arguments<sup>/9/</sup> that the former is not the case.

Thus, the inclusion of the residual interaction seems to be unavoidable. This statement is also confirmed by a larger success of exciton-model-type calculations for angle-integrated spectra (compare, e.g. ref.<sup>/10/</sup>). On the other hand, the exciton models for fast particle emission in heavy ion reactions are far from being completely worked out and mostly highly inconsistent with existing models for calculating heavy ion trajectories, particle transfer, etc...

Up to now there is only one fundamental approach allowing to treat the mechanism of energy dissipation and other dynamical features of a heavy ion reaction consistently with light particle emission. This is the time-dependent mean-field theory (TDHF) including its extensions for taking into account the residual interaction (see, e.g.<sup>/11,12/</sup> and references cited therein). However, due to the large computer times needed for a realistic calculation of fast particle emission even in the framework of the standard TDHF initial value problem (without two-body collisions) there is only a small number of such investigations<sup>/13-16/</sup>.

In TDHF fast particles are identified with a low-density component emerging in forward direction at a typical time of 1-2 times the transit time (several  $10^{-22}$  s) of a nucleon of the projectile across the recipient nucleus and characterized by a broad velocity distribution involving components much higher than the beam velocity. To this extent they very much resemble PEP discussed above. However, in TDHF there is no explicit assumption of a strong coupling of relative to Fermi motion as it is in the Fermi-jet model. Contradictorily results of refs.<sup>/13,14/</sup> and ref.<sup>/16/</sup> concerning the strength of this coupling have been shown to be probably related to spurious PEP which are connected with an insufficient numerical stability<sup>/17/</sup>. It turns out that relative and intrinsic motion are really much weaker coupled than it is assumed in the Fermi-jet models. PEP appearing in a TDHF evolution can only be responsible for a small fraction (if at all) of the energetic nucleons observed in experiment<sup>/17/</sup>. This conclusion is in agreement with that of refs.<sup>/8,9/</sup> mentioned above.

In the present paper it is shown that

i) the PEP's usually investigated in TDHF are only the first, most energetic portion of particles emitted in the course of a TDHF evolution.

ii) The total yields of PEP's in TDHF are strongly correlated with the binding energy of the last nucleon in the projectile. This finding is in disagreement with experimental data and once more confirms the conclusion of ref.<sup>/17/</sup> of a small weight of Fermi-jet-type particles in the high-energy tails of the nucleon spectra.

iii) The projectile incident on the target excites large amplitude oscillations of either the compound system or the separating fragments which in turn decay by particle emission.

These conclusions are drawn from numerical results for effectively one-dimensional slab collisions. The model (originally developed in ref.<sup>/18/</sup>) and numerical details including remarks on numerical stability of the particle-emission results are described in refs.<sup>/17,19/</sup>.

## II. A VERY ASYMMETRIC SLAB COLLISION

For methodological reasons we first prefer to analyze a very asymmetric ( $A_p = 0.2 \text{ fm}^{-2}$ ,  $A_t = 2.0 \text{ fm}^{-2}$ ) slab collision at not too high incident energy ( $E/A_{\text{lab}} = 5 \text{ MeV}$ ). In this case the projectile slab is described by only one single-particle wave function  $\phi_p(z,t)$  (compare slab mass tables given in refs.<sup>/18,19/</sup>). At the given incident energy fusion occurs and the target/composite-system mean-field does not very drastically change in time due to a comparably small distortion of the target mean-field by the projectile slab. So, in a crude, qualitative sense, the example under consideration very much resembles the problem of an initial wave packet interacting with a (nearly constant) potential well. On the other hand, it mimics a very asymmetric heavy ion reaction.

In fig. 1 the time evolution for the total single particle density of the problem as well as for the partial density

$$\rho_p = A_p |\phi_p|^2 \quad (1)$$

initially representing the projectile slab are shown.

The initial wave packet evolves mostly in qualitative agreement with our expectations for the corresponding single-particle problem in a constant external potential. Only at later times the target nucleons come increasingly into play:

i) When entering the target potential region a small fraction of the wave packet is reflected backwards (compare  $\rho_p$  at  $t = 60 \text{ fm/c}$  and  $120 \text{ fm/c}$ ).

ii) Having reached the forward edge of the potential a small fraction of the wave packet is transmitted (density lump emerging around



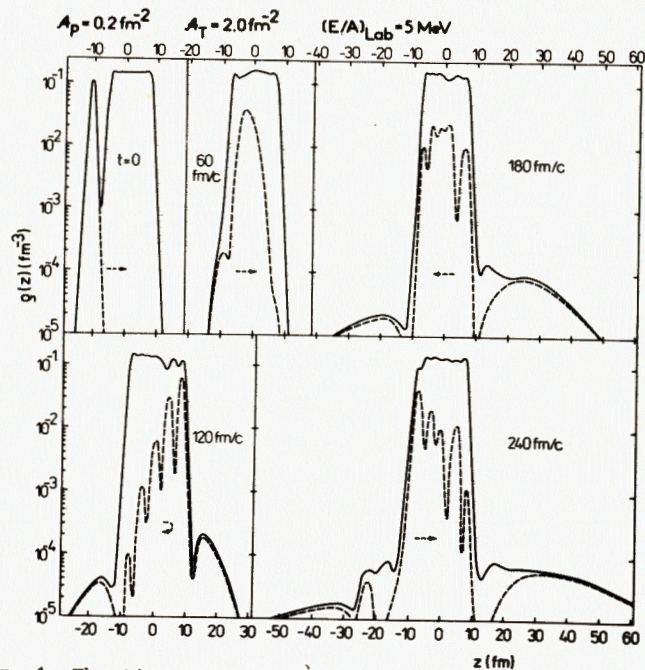


Fig. 1. The time evolution of the total single-particle density  $\rho(z, t)$  (full lines) as well as that part  $\rho_p$  of it which initially describes the projectile (dashed lines), i.e. which illustrates the time evolution of the initial wave packet in the composite system.

$z = 17$  fm at  $t = 120$  fm/c) while the remaining part becomes reflected exhibiting a typical diffraction-pattern resulting from interferences between reflected and not yet reflected components ( $t = 120$  fm/c).

iii) At its way back the wave packet becomes increasingly distorted. This is not only an effect of the finiteness of the target potential but also of some time-dependent oscillations of the composite-system mean-field. The transmitted and reflected portions of the wave packet go away (compare  $t = 180$  fm/c) from the composite system exhibiting substantial dispersion in space which indicates broad velocity distributions.

iv). The reflection from the left-hand edge of the potential is connected with a further transmission (backwards) of some part of the wave packet being already smaller in amplitude as compared to the portion transmitted forwards ( $t = 240$  fm/c).

v) The wave packet continues to bounce between the edges of the common potential well. It becomes increasingly deformed and periodically pushes out some small density lumps of decreasing amplitude. Increasingly wave functions of the target are involved in the emitted fractions of density (see the small maxima in the total density outside the composite system at  $t = 180$  fm/c,  $t = 240$  fm/c which are not correlated with a corresponding peak in  $\rho_p$ ). That is, a collective large amplitude density oscillation is generated which becomes damped by particle emission. Although it does not represent a stationary state, its main components can seemingly be related to periods around  $T \approx 200$  fm/c corresponding to  $\hbar\omega \approx 6.2$  MeV. Admixtures of higher  $\hbar\omega$  are, of course, also present allowing particle emission with energies of the order and even larger than the incident energy per nucleon. Density profiles for instants later than  $t = 240$  fm/c are not shown in fig. 1 since even in the given large numerical base of length 180 fm interactions with the reflecting edges of the box increasingly deform the low density tails (compare ref.<sup>/17/</sup>).

In connection with the observed large amplitude density oscillations in the present one-dimensional study we mention a more realistic TDHF investigation of vibrational spectra of a post grazing collision  $^{40}\text{Ca}$  nucleus performed in ref.<sup>/20/</sup>. In that work the time evolution of moments of the density of the type  $\langle X^n Y^m Z^p \rangle$  have been recorded and then Fourier-analysed. The result was a very broad, clearly structured frequency spectrum ranging up to 75 MeV (region considered in that paper) and probably even higher. For more deep inelastic events the corresponding Fourier-transform exhibited the same energy spectrum but with much smaller intensity for the high-frequency modes  $\hbar\omega \gtrsim 30$  MeV despite the larger average excitation of the fragment. This indicates the structures being created preferentially in grazing rather than deep inelastic collisions. These results are in qualitative agreement with experimental results of ref.<sup>/21/</sup> for near grazing collision of  $^{40}\text{Ca} + ^{40}\text{Ca}$  at  $E_{\text{Lab}} = 400$  MeV indicating structure in the excitation spectrum of the residual nuclei at energies that at first glance are much higher than seems appropriate (25, 50, 80, 120, 150 MeV). Most of the peaks (despite some exceptions) observed in the TDHF calculations could be grouped in multiples of some lower-energy components<sup>/20/</sup>. So, it was not quite clear whether or not this indicates multiple phonon effects, effects of the non-linearity of the TDHF equations, or primary large amplitude collective excitations. Recent experiments<sup>/22/</sup> with different (asymmetric) systems and a better energy resolution have shown evidence for an even more complex spectrum. These structures could successfully be interpreted in terms of target



multi-phonon excitations built for a large part with the giant quadrupole isoscalar phonon (GQR)<sup>/22,23/</sup>.

Returning to the discussion of our one-dimensional results we emphasize that in this model only compressional density oscillation modes are possible<sup>/18/</sup>, i.e. in comparison with realistic TDHF calculations there is only a very poor number of degrees of freedom described essentially by 7 complex functions  $\phi;(\mathbf{r},t)$  in the present example. So, it is not unexpected that in any slab collision such large amplitude density oscillations are excited and can survive while its "realistic modifications" can be observed only in grazing collisions or probably serve as doorway states at smaller impacts decaying on a fast time scale into more complicated states (thermalization). Our one-dimensional results on particle emission after PEP emission are thus to be understood as indicating a substantial width of these modes also due to light particle emission. The damping of nuclear monopole vibrations in TDHF (effectively one-dimensional problem) due to particle emission was investigated in ref.<sup>/24/</sup>.

A last remark to fig. 1 concerns the fraction of projectile density reflected after the projectile is entering the target potential. There is no experimental hint on the existence of such particles, i.e. on some more or less pronounced backward peak in the generally forward-peaked angular distributions at high emission energies for very asymmetric collisions. Probably this is an artifact of the mean-field approximation although its existence is plausible by the discussion given above. Certainly, the inclusion of residual interactions would make the system sufficiently viscous to suppress this phenomenon. It is also obvious that the reflected fraction will decrease with increasing incident energy while the transmitted part (PEP) will increase<sup>/17/</sup>. The incident energy in our example just represents the energy (above the Coulomb barrier, which is zero for slab collisions) at which substantial fast particle emission sets in<sup>/10/</sup>. Furthermore, for decreasing asymmetry in slab collisions there is an increasing amount of PEP from the target covering the reflected portion from the projectile (this becomes obvious for symmetric collisions). This was one of the reasons of the special choice of extreme asymmetry. Moreover, if rescaling the slab thicknesses  $A_{p,T}$  (number of nucleons per unit area) to mass numbers  $A_{p,T}$  of realistic nuclei by taking the half widths of the slab densities to be the nuclear diameters<sup>/18/</sup> ( $A_{p,T} = 2r_0 A_{p,T}^{1/3} \rho_0$  - for not too small  $A$ ) the present slab collision would correspond to an unrealistic mass asymmetry of  $A_T/A_P \approx 1000$ . Obviously, in real experiments this ratio is much less. So, an  $\alpha$ -particle would correspond to  $A \approx 0.55 \text{ fm}^{-2}$  and the target slab of

our example would correspond to  $A_T \approx 200$ . Hence, in any case it is more or less impossible to obtain a fraction of fast reflected particles in experiments in order to test corresponding predictions of TDHF which in turn are probably very small and surely hard to be separated from target PEP in the theory.

### III. SHELL EFFECTS IN THE TOTAL YIELD OF PEP

We now return to a more detailed investigation of the first transmitted fraction of particles (PEP) and try to support by physical arguments the formal statement of ref.<sup>/17/</sup> (made on the basis of a numerical stability study) of such an emission mechanism having a quite small weight in the experimentally observed fast particle yields.

PEP in TDHF (as well as in the Fermi-jet model) emerge at an early instant only slightly larger than the transit time of a projectile nucleon across the target nucleus. Hence, they are injected into the recipient immediately after the nuclei touch and still preserve their individuality to a large extent (small overlap). In such a picture one should expect a significant dependence of the total yields of PEP on the binding energy of the last particle in the donor nucleus.

In order to investigate quantitatively this point, we have performed a large number of slab-collision calculations fixing the target  $A_T = 2.0 \text{ fm}^{-2}$  as well as the incident velocity (energy per nucleon) but varying the projectile slab thickness in a broad range from  $0.2 \text{ fm}^{-2}$  to  $2.0 \text{ fm}^{-2}$ .

In fig. 2 for incident energy  $(E/A)_{\text{lab}} = 5 \text{ MeV}$  the total yield  $\Delta A_p$  of PEP from the projectile divided by the projectile slab thickness  $A_p$ , i.e. the percentage of the projectile nucleons being emitted as PEP, is plotted against the slab thickness of the projectile. The partial contribution of nucleons from the highest orbital in the projectile is also plotted. For comparison a simple Fermi-gas estimate for the corresponding three-dimensional system, calculated as described in ref.<sup>/25/</sup>, is shown. On the same footing Fermi-gas estimates modified for our slab geometry (cylindrical Fermi surfaces) are included in the figure:

$$\left(\frac{\Delta A}{A}\right)_p = \left(\frac{A_T}{A_T + A_p} \sqrt{\frac{(E/A)_{\text{lab}}}{E_F}} - \sqrt{1 + \frac{|B_T|}{E_F} + 1}\right) \cdot \frac{1}{2}. \quad (2)$$

The monotonic decrease of the Fermi-gas estimate values of  $\Delta A/A$  with increasing  $A_p$  expresses simply the fact that for heavier projectiles a larger part of the incident kinetic energy goes into the center of mass motion and, therefore, is not available for PEP formation. On the average the TDHF PEP yields follow the trend of the Fermi-gas estimate



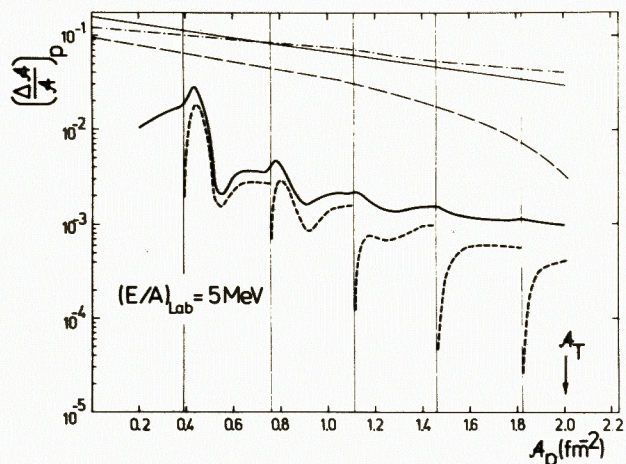


Fig. 2. Percentage of the projectile nucleons  $(\Delta A/A)_p$  being emitted in a collision with a thick  $A_T = 2.0 \text{ fm}^{-2}$  target slab at incident energy 5 MeV/A (full lines). The dashed lines denote the contribution to  $(\Delta A/A)_p$  only from the highest occupied orbital of the projectile. The vertical lines mark the position of "closed shells". The thin monotonic lines above represent several simple Fermi-gas estimates: for the corresponding three-dimensional collision with  $B_T = 8 \text{ MeV}$ ,  $E_F = 38 \text{ MeV}$  (full line), and one-dimensional Fermi-gas estimates using eq. (2) with  $B_T = 8 \text{ MeV}$  (dash-dotted line), and  $B_T = 14.4 \text{ MeV}$  (dashed line) which has been determined from the target ground state total energy per unit area  $E_T/\Omega$  divided by the target slab thickness.

tes, the absolute values being substantially smaller due to geometrical restrictions not included in the simple Fermi-gas phase space model and a non-ideal coupling of intrinsic to relative motion in TDHF as discussed above.

In order to understand the pronounced structures in the total PEP yield curve as a function of projectile slab thickness one has to compare with the slab mass table shown in fig. 3. It is seen that the position of "magic" slabs is nearly equidistant, i.e. does not compare with the shell structure of realistic nuclei. Even more important for the following discussion is the observation that the last particle is most loosely bound for "magic" slabs while this binding is stronger in between "closed shells". This feature of one-dimensional slabs is directly opposite to the situation in real nuclei. The terminology "magic slab" and "closed shell" should be used, however, with caution since in the slab geometry there are no gaps between the discrete (in Z-direction) states<sup>/18/</sup>. For a

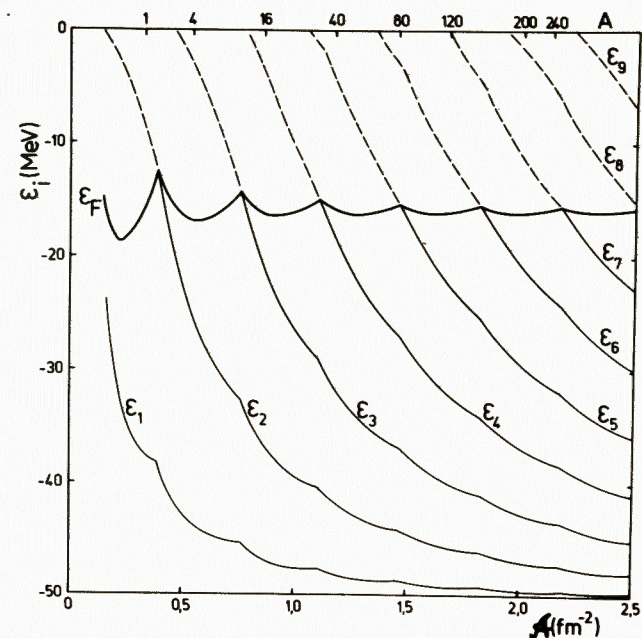


Fig. 3. The slab mass table for the simplified Skyrme force used in ref.<sup>/17/</sup>. The A-dependence of the single-particle energies  $\epsilon_i$ ; (solid lines - occupied, dashed lines - unoccupied levels) and the Fermi energy  $\epsilon_F$  (heavy line) is shown. The upper abscissa is labelled by the three-dimensional equivalent mass number.

given A nucleons with any energy up to the Fermi energy exist due to the transverse motion described by plane waves.

From this it is not unexpected that in fig. 1 the PEP yields are larger for "magic slabs" than for slabs in between "closed shells". The fact that the structures in fig. 2 decrease with increasing  $A_p$  clearly correlates with a similar behaviour of the Fermi energy in fig. 3. Particles from the highest orbitals are preferred for PEP emission (dashed curves in fig. 2). The peaks of the PEP yield are still slightly shifted from the "closed shells" to the right since the occupation number for the new highest discrete orbital is still zero for "magic slabs" and must somewhat increase with slightly increasing A to give a maximum in  $\Delta A/A$ . This situation is similar to realistic cases when one adds a single nucleon to a closed shell - since it is loosely bound it can be emitted more easily. The difference is that in slab geometry the occupation numbers change continuously from zero to values smaller than unity with increasing A.

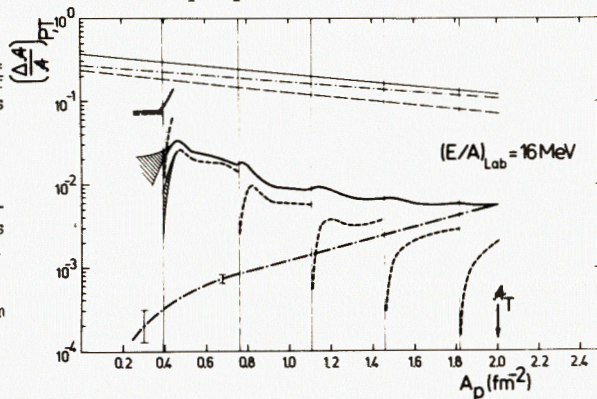


Independently of the specifics of the slab-geometry we claim that the observed strong correlation between the total PEP yield and the binding energy of the last particle is a general feature of TDHF dynamics.

At a higher incident energy one expects intuitively less pronounced shell effects in the fast particle yields. To proof this, we have performed a second series of slab collisions of 16 MeV/A incident energy. The results shown in fig. 4 support this expectation.

At this energy there is an ambiguity in the determination of the

Fig.4. The same as in Fig.2 but for  $(E/A)_{\text{lab}} = 16$  MeV. The ratio of target-like PEP yields to the target slab thickness  $(\Delta A/A)_T$  is also shown (thick dot-dashed line). Error bars and hatched regions denote ambiguities in extracting  $(\Delta A/A)_T$  values at very small densities, and in separating the fast from the slower PEP component (see text), respectively.



projectile-like PEP around  $A_p \approx 0.46 \text{ fm}^{-2}$ . For smaller values of  $A_p$  the density shape of the PEP exhibits two components similar to the case illustrated in fig. 4 of ref. /17/. The slower component with a mean velocity close to the projectile velocity also disperses in space at later times as it is characteristic for the faster component. They are hard to separate. In fig. 4 for  $A_p < 0.46 \text{ fm}^{-2}$  the hatched regions refer to the faster PEP component only. Slightly above  $A_p = 0.46 \text{ fm}^{-2}$ , however, the central density of the slower component grows in time so that it is to be identified with a first fragment rather than with PEP and is not further included into the PEP yields at higher  $A_p$ .

The target-like PEP yields are also shown in fig. 4. There is no structure obtained. The same holds also at the lower incident energy of fig. 2 (not shown there). This curve can be interpreted also in the following way: For a fixed projectile and fixed incident velocity the projectile-like PEP smoothly depend on the target mass number. The smaller the target is the less PEP emerge. This can be understood already from geometry (at least in the present case of a heavy projectile colliding with smaller targets).

The lack of structure in the target-like PEP yields together with the structures in the projectile-like PEP strongly correlating with the binding energy of the last nucleon in the projectile clearly emphasize that in TDHF PEP are injected into the recipient very early and then more or less freely propagate through the target underlying some quantum diffraction in the finite target potential. After being injected the fraction of them which is transmitted smoothly depends on the size of the target potential well.

Exactly the same problem we were dealing with in this section was attacked experimentally in ref. /26/: Neutron spectra in coincidence with fusion residues at several angles have been measured for  $^{12}\text{C}$  and  $^{13}\text{C}$  incident on  $^{158}\text{Gd}$  and  $^{157}\text{Gd}$ , respectively, at energies around 12 MeV/A. Owing to the fact that the difference in the neutron binding energies in  $^{12}\text{C}$  and  $^{13}\text{C}$  amounts to  $\Delta B_n = 13.8$  MeV these projectiles should be most appropriate to look for correlations in the fast particle yields with binding energies. However, the authors of ref. /26/ did not find any significant dependence of a high energy tail of the neutron spectra (attributed to non-equilibrium emission) on the binding energy of the last neutron in the projectile.

This experimental finding is in contradiction with our TDHF result: A change in the binding energy of the last nucleon by about 5 MeV leads to a change in the PEP yields by more than one order of magnitude at incident energy 5 MeV/A (compare figs. 2 and 3). For an incident energy even higher than in the experiment of ref. /26/ still a considerable effect has been found (fig. 4) of roughly a factor of 2.

From this we draw the conclusion that the Fermi-jet mechanism (even if quantum diffraction is not neglected like in TDHF) can be responsible only for a very small fraction of the particles observed in experiment. Most of the donor nucleons after being injected into the target should be rescattered via the residual interaction with target nucleons losing in this way their "memory" with respect to the shell structure of the projectile but still being fast enough to be able to contribute to the high-energy tails of the nucleon spectra including also larger angles.

Moreover, there are other possible mechanisms proposed in the literature which predict non-evaporative particle emission either without injection of nucleons from the donor to the recipient (IEP - ref. /4/), or even in the final stage of the heavy ion reaction long after thermal equilibrium is established ("neck particles" /27,28/, "catapult particles" and corresponding exciton cascades initiated after scission in the final fragments /29/).



## REFERENCES

1. Bondorf J.P. et al. Phys.Lett., 1979, 84B, p. 163;  
Bondorf J.P. et al. Nucl.Phys., 1980, A333, p. 285.
2. Sebille F., Remaud B. Z.Phys., 1983, A310, p. 99.
3. Tricoire H. Z.Phys., 1983, A312, p. 221.
4. Tricoire H. Z.Phys., 1984, A317, p. 347.
5. Yoshida Sh. Z.Phys., 1982, A308, p. 133.
6. Otsuka T, Harada K. Phys.Lett., 1983, 121B, p. 106.
7. Blann M. Phys.Rev., 1981, C23, p. 205.
8. Brosa U., Krone W. Phys.Lett., 1981, 105B, p. 22.
9. Brosa U. Proceedings of the International Workshop on Gross Properties of Nuclei and Nuclear Excitations XI, Hirscheegg, 1983, p. 87.
10. Holub E. et al. Phys.Rev., 1983, C28, p. 25w.
11. Negele J.W. Rev.Mod.Phys., 1982, 54, p. 913.
12. Mädler P. Particles and Nuclei, 1984, 15, p. 418 (in Russian).
13. Devi K.R.S. et al. Phys.Rev., 1981, C24, p. 2521.
14. Dhar A.K. et al. Phys.Rev., 1982, C25, p. 1432.
15. Stocker H. et al. Phys.Lett., 1981, 101B, p. 379.
16. Drozd S., Okolowicz J., Ploszajczak M. Phys.Lett., 1983, 121B, p. 297.
17. Mädler P., Z.Phys., 1984, A318, p. 87.
18. Bonche P., Koonin S.E., Negele J.W. Phys.Rev., 1976, C13, p. 1226.
19. Mädler P., Nikishov P.Yu., Zakhariev B.N. JINR Communication E4-84-487, Dubna, 1984.
20. Flocard H., Weiss M.S. Phys.Lett., 1981, 105B, p. 14.
21. Frascaria N. et al. Z.Phys., 1980, A294, p. 167.
22. Chomaz Ph. et al. Preprint IPNO/TH 84-85, Orsay, July 1984.
23. Chomaz Ph., Vautherin D. Phys.Lett., 1984, 139B, p. 244.
24. Stringari S., Vautherin D. Phys.Lett., 1979, 88B, p. 1.
25. Davies K.T.R. et al. Preprint MAP-23, 1982.
26. Gavron et al. Phys.Rev., 1981, C24, p. 2048.
27. Brosa U., Grossmann S. Proceedings of the International Workshop on Gross Properties of Nuclei and Nuclear Excitations XI, Hirscheegg, 1983, p. 187.
28. Brosa U., Grossmann S. J.Phys., G, 1984, 10, p. 933.
29. Mädler P. submitted to Z.Phys. A.

Received by Publishing Department  
on October 26, 1984.

Мэдлер П.

E7-84-690

Об испускании частиц в зависящем от времени  
приближении Хартри-Фока

Исследуется испускание быстрых частиц в приближении зависящего от времени среднего поля /ЗВХФ/ для столкновения одномерных ядерных слоев. Для фиксированных мишени и начальной скорости полные выходы частиц как функции массового числа налетающего ядра сильно коррелируют с энергией связи последнего нуклона налетающего ядра. Это явно противоречит эксперименту. Следовательно, механизм фермиевских струй не может отвечать за большинство быстрых частиц, обнаруженных в экспериментах, даже, если учесть квантовую дифракцию /как в ЗВХФ/. Найдено, что колебания плотности с большой амплитудой, которые являются единственными модами возбуждения в ЗВХФ в данной геометрии, затухают за счет дальнейшего испускания частиц.

Работа выполнена в Лаборатории теоретической физики ОИЯИ.

Сообщение Объединенного института ядерных исследований. Дубна 1984

Mädler P.

E7-84-690

On Particle Emission in TDHF Approximation

Investigations of fast particle emission in the time-dependent mean-field approximation (TDHF) have been performed for one-dimensional slab collisions. For a fixed target mass number and incident velocity the total yields of PEP exhibit pronounced structures as a function of the projectile mass number, which strongly correlate with the binding energy of the last nucleon in the projectile. This is in explicit disagreement with experiment. The conclusion has been drawn that the Fermi-jet mechanism cannot be responsible for most of the fast particles observed in experiment, even if quantum diffraction is taken into account (as in TDHF). After PEP emission large amplitude density oscillations, which are the only possible modes in the slab geometry, are found to be damped by further particle emission.

The investigation has been performed at the Laboratory of Theoretical Physics, JINR.

Communication of the Joint Institute for Nuclear Research. Dubna 1984